

SUMMARY

In this paper angle dependent reflectivity is retrieved in the presence of dip by means of prestack migration. We start with reviewing the downward extrapolation process and show how angle dependent reflectivity can be extracted via the *generalized imaging* principle. Next, in a simple example with a constant-dip reflector, we demonstrate that the angle dependent reflection curves are shifted over a distance equal to the magnitude of the dip. In practice, local dip-angle information should be extracted from the structural image by using the *conventional imaging* principle. This dip information should be taken into account in the final result, yielding a correctly positioned angle dependent reflection coefficient curve for each grid point of interest.

Imaging angle dependent reflectivity via prestack migration appears a rigorous alternative to AVO related methods, particularly in geologically complex structures. Amplitude information for each grid point (depth point), directly obtained as a function of angle (AVA) or ray parameter, can be used for subsequent stratigraphic and lithologic inversion in a target zone.

INTRODUCTION

Seismic migration techniques generally aim at resolving *structural* information from seismic data. By using the conventional imaging principle, an *average* reflection coefficient per grid point (depth point) is determined (Claerbout, 1976). De Bruin et al. (1988) show that prestack migration can also yield the *angle dependent reflection coefficient* per subsurface depth point by generalizing the imaging principle. For the sake of efficiency the imaging for angle dependent reflectivity (ADR) may only be performed in an area of interest, which we call the target zone.

Thus far we illustrated the retrieval of angle dependent reflection coefficients from simulated data with horizontally layered subsurface models (De Bruin et al., 1988). Hence the transformation from ray parameter p to angle α is simply given by $p = \sin\alpha/c$, where c is the velocity just above the reflector of interest. However, as the extraction of ADR is based on prestack migration in the frequency-space domain (Berkhout, 1985), *any* subsurface geometry can be handled. The procedure for

imaging angle dependent reflectivity for laterally varying media is the same as for the 1-D case. Only the *local* dip at each subsurface depth point on a (curved) reflector must be known in order to interpret the imaged results correctly. This is an important advantage over AVO, where various problems are encountered when dips are present (see Resnick et al., 1987).

NOTATION

In this paper the matrix notation is used as introduced by Berkhout (1985). The traces of all shot records $p(x_m, x_n, z_0, t)$ i.e. wave fields with source position at x_n , receiver position at x_m measured as a function of time t at acquisition depth level z_0 , are Fourier transformed to the frequency domain, yielding $P(x_m, x_n, z_0, \omega)$. In this domain all seismic prestack data are gathered per frequency component ω_j and put into a matrix, denoted by $P(z_0)$. Each matrix has the monochromatic common shot gathers in the columns and the monochromatic common receiver gathers in the rows. So each element P_{mn} of the data matrix P (m^{th} row, n^{th} column) defines the response of source position n at receiver position m for the frequency component ω_j . The superscripts $+$ and $-$ correspond to downgoing and upgoing waves, respectively.

MULTI-OFFSET MIGRATION FOR ANGLE DEPENDENT REFLECTIVITY

ADR can be retrieved from decomposed elastic multi-source, multi-offset data by prestack migration. Hence, each subsurface depth point of interest is illuminated under a range of angles of incidence. In this section the retrieval of ADR is briefly summarized. For a more rigorous treatment the reader is referred to De Bruin et al. (1990).

Following Berkhout (1985), after decomposition and surface multiple elimination the monochromatic upgoing primary multi-offset data $P^-(z_0)$ at the surface can be simply represented with:

$$P^-(z_0) = X(z_0) S^+(z_0), \tag{1}$$

where $S^+(z_0)$ contains one Fourier component of all downgoing source wave fields at z_0 and $X(z_0)$ one Fourier component of the

subsurface transfer function. For primary information $X(z_0)$ is a combination of downward propagation W^+ , reflection R and upward propagation W^- for each reflection boundary. In formulation:

$$X(z_0) = \sum_i [W^-(z_0, z_i) R(z_i) W^+(z_i, z_0)]. \quad (2)$$

In the migration procedure we have to determine reflectivity R , assuming that the seismic measurements $F^-(z_0)$, the source $S^+(z_0)$ and a macro subsurface model are given. First we determine $X(z_0)$ in equation (1) by deconvolving for the source wave field. The next step is a compensation for the propagation effects in $X(z_0)$ in equation (2) for each depth level. The propagation effects between the surface and depth level z_k can be eliminated by

$$X(z_k) = F^-(z_k, z_0) X(z_0) F^+(z_0, z_k), \quad (3a)$$

where the inverse extrapolation operators are defined as follows:

$$F^-(z_k, z_0) \triangleq [W^-(z_0, z_k)]^{-1} \approx [W^+(z_k, z_0)]^*, \quad (3b)$$

and

$$F^+(z_0, z_k) \triangleq [W^+(z_k, z_0)]^{-1} \approx [W^-(z_0, z_k)]^*, \quad (3c)$$

(see Berkhout, 1985). The final step is imaging. Therefore we rewrite (3a) by substituting (2), yielding

$$X(z_k) = R(z_k) + \sum_{i \neq k} [F^-(z_k, z_0) W^-(z_0, z_i) R(z_i) W^+(z_i, z_0) F^+(z_0, z_k)]. \quad (4)$$

Imaging for *structural information* involves

$$\langle R(z_k) \rangle = \frac{\Delta \omega}{2\pi} \sum_{\omega} X(z_k), \quad (5)$$

where only the diagonal elements of estimation $\langle R(z_k) \rangle$ are selected. (Bear in mind that summing over all frequency components is equivalent to Inverse Fourier Transforming and selecting the $t = 0$ component). These diagonal elements represent the ZO reflection coefficients at each grid point of

depth level z_k .

For imaging ADR (see De Bruin et al., 1988), the frequency contributions must be summed along lines of constant ray parameter at each grid point (x_m, z_k) . This yields a true amplitude estimate of the ADR:

$$\bar{R}_m(z_k, p) = \frac{1}{N_{\omega}} \sum_{\omega} \bar{X}_m(z_k, \omega; p), \quad (6)$$

where N_{ω} is a correction for the frequency content of the wavelet. $\bar{X}_m(z_k, \omega; p)$ denotes the response at grid point (x_m, z_k) in the frequency - ray parameter $(\omega-p)$ domain, obtained by spatial Fourier transforming the m^{th} row of matrix $X(z_k)$:

$$\bar{X}_m(z_k, \omega; p) = \Delta x \sum_n X_m(z_k, \omega, (m-n)\Delta x) e^{j\omega p(m-n)\Delta x}. \quad (7)$$

The whole procedure is repeated for each extrapolation depth level, yielding a p - z panel for each lateral position x_m .

ANGLE DEPENDENT REFLECTIVITY IN THE PRESENCE OF DIP

In the presence of dip we still perform the same procedure for imaging ADR as with horizontal interfaces. Consider the simple situation with a constant-dip reflector (Figure 1). When a (plane) wave immerses on subsurface depth point (x_m, z_k) with immergence angle α (measured with respect to the vertical), the true immergence angle at this point on the dipping reflector is: $\delta + \alpha$. For a dipping reflector the dip-angle at each subsurface depth point on the reflector has to be taken into account for the correct interpretation of the angle dependent reflection coefficient. The structural image should provide the dip-angle δ .

EXAMPLE

The model that is used in this example contains an interface with a 10 degree dip over a velocity contrast of 1500 m/s and 3000 m/s. (Figure 2). For this example 256 shot records were modeled with 256 receivers with 10 m shot and receiver spacing. In Figure 3 five shot records are plotted. All shot records were used for the migration. For the macro model a

homogeneous subsurface was taken with a velocity of 1500 m/s. Beside the extraction of ADR, a structural section is retrieved as well by conventional imaging. The migrated section, consisting of the average reflection coefficients, is shown in Figure 4a. Note that the dip is imaged as expected (compare with the true model in Figure 4b).

We also indicated three vertical positions along which the ADR is determined for each extrapolation level. The three p-z panels are displayed in Figure 5 for lateral positions 630 m, 1270 m and 1910 m. Obviously only an ADR image is obtained when the interface is crossed. If we pick the amplitude along the images, the angle dependent reflection coefficients are obtained. The results are depicted in Figure 6 for the three intersection points. The ADR curves have been shifted up dip over a distance equal to the magnitude of the dip.

In case of a strong contrast, like in this example, it is even possible to estimate the dip-angle from the ADR curves of Figure 6 by looking at the position of the local minimum. In practical situations, however, the contrasts will be often smaller and determining the position of the minimum is not that reliable any longer. But, as we also have the structural image (Figure 4a), the dip information should come from this result. During the presentation we will discuss an example for a complex overburden.

CONCLUSIONS

ADR can be retrieved from seismic data by means of prestack migration. Often we are only interested in the detail of a specific area of the subsurface (the target zone). Per target grid point the angle dependent reflection coefficient can be obtained by applying the *generalized* imaging principle after the downward extrapolation process. As the downward extrapolation is performed in the frequency-space domain, *any* complex subsurface can be handled.

We have illustrated that ADR can be retrieved from simulated seismic data for a simple 2-D medium with a constant-dip reflector. We have seen that the ADR results are shifted over a distance equal to the magnitude of the dip. Hence, ADR results in case of laterally varying media can be interpreted correctly when the (local) dip is known. This information should be extracted from the structural image (average reflectivity). The proposed method can be referred to as 'depth point related

AVA'. It has a big advantage compared to midpoint related AVO techniques where various problems arise in case of laterally varying media. A more complex example will be discussed during the presentation.

REFERENCES

- Berkhout, A.J., 1985, Seismic migration, Volume A, Theoretical aspects: Elsevier, Amsterdam - New York.
- Claerbout, J.F., 1976, Fundamentals of Geophysical Data Processing: McGraw-Hill Book Co.
- De Bruin, C.G.M., Wapenaar, C.P.A., and Berkhout, A.J., 1988, Angle-dependent reflectivity by shot record migration: Presented at the 58th Ann. Mtg. Soc. Exp. Geophys., Expanded Abstracts, 1093-1096.
- De Bruin, C.G.M., Wapenaar, C.P.A., and Berkhout, A.J., 1990, Angle dependent Reflectivity by Prestack Migration: Geophysics, September issue.
- Resnick, J.R., Ng. P., and Larner, K., 1987, Amplitude Versus Offset in the Presence of Dip: Presented at the 57th Ann. Mtg. Soc. Exp. Geophys., Expanded Abstracts, 617 - 620.

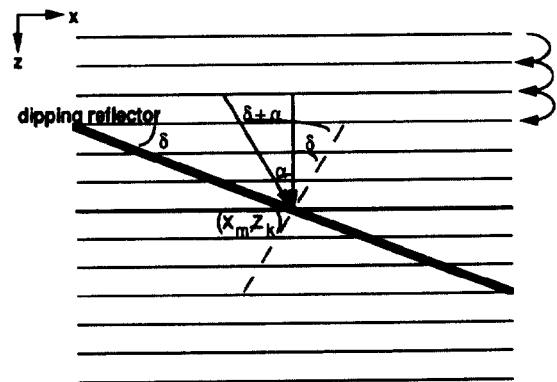


Figure 1
Immergence angle in case of dip: whereas the angle of incidence at point (x_m, z_k) on a horizontal interface is α , on the dipping reflector the angle of incidence is $\alpha + \delta$, where δ is the dip angle.

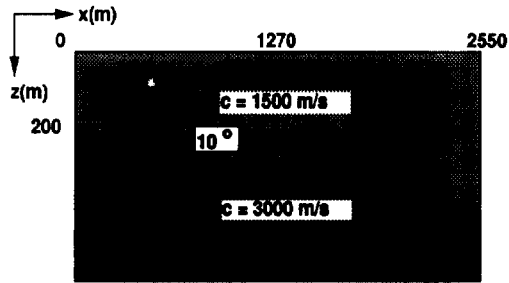


Figure 2
Acoustic subsurface model with a 10 degree dipping interface over a velocity contrast.

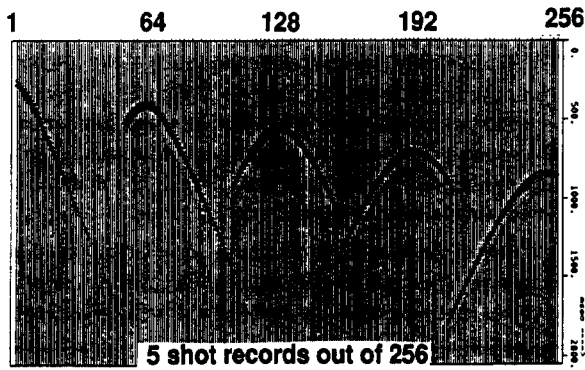


Figure 3
Input data for the model of Figure 2: 5 shot records out of the 256 shot records.

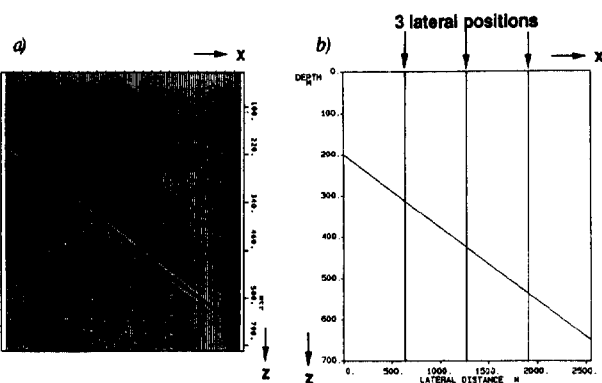


Figure 4
a) Migrated section: ZO reflection coefficient computed per grid point.
b) Correct subsurface model. The three arrows indicate the lateral positions along which the ADR images are computed.

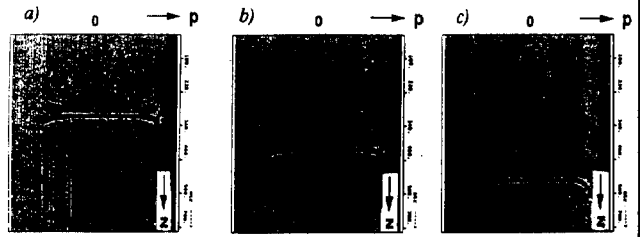


Figure 5
ADR panels: ray parameter versus depth for the three lateral positions indicated in Figure 4b.
a) at $x = 630$ m, b) at $x = 1270$ m, c) at $x = 1910$ m.

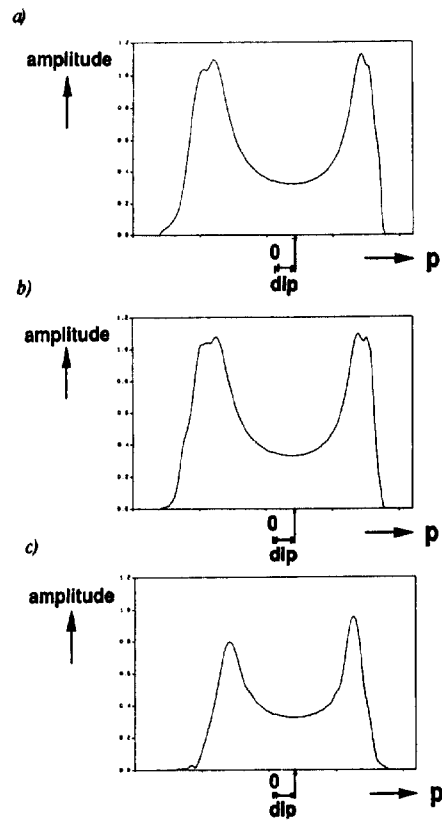


Figure 6
Angle dependent reflection coefficients for the three intersection points with the dipping interface: obtained by picking the amplitudes in Figure 5. Note the up-dip shift corresponding with dip-angle $\delta = 10^\circ$:
a) at $x = 630$ m, b) at $x = 1270$ m, c) at $x = 1910$ m.